

A New Species of Baleen Whale (Isanacetus-Group) from the Early Miocene, Japan

Authors: Kimura, Toshiyuki, Hasegawa, Yoshikazu, and Suzuki, Tadashi

Source: Paleontological Research, 27(1) : 85-101

Published By: The Palaeontological Society of Japan

URL: <https://doi.org/10.2517/PR210009>

The BioOne Digital Library (<https://bioone.org/>) provides worldwide distribution for more than 580 journals and eBooks from BioOne's community of over 150 nonprofit societies, research institutions, and university presses in the biological, ecological, and environmental sciences. The BioOne Digital Library encompasses the flagship aggregation BioOne Complete (<https://bioone.org/subscribe>), the BioOne Complete Archive (<https://bioone.org/archive>), and the BioOne eBooks program offerings ESA eBook Collection (<https://bioone.org/esa-ebooks>) and CSIRO Publishing BioSelect Collection (<https://bioone.org/csiro-ebooks>).

Your use of this PDF, the BioOne Digital Library, and all posted and associated content indicates your acceptance of BioOne's Terms of Use, available at www.bioone.org/terms-of-use.

Usage of BioOne Digital Library content is strictly limited to personal, educational, and non-commercial use. Commercial inquiries or rights and permissions requests should be directed to the individual publisher as copyright holder.

BioOne is an innovative nonprofit that sees sustainable scholarly publishing as an inherently collaborative enterprise connecting authors, nonprofit publishers, academic institutions, research libraries, and research funders in the common goal of maximizing access to critical research.

A new species of baleen whale (*Isanacetus*-group) from the early Miocene, Japan

TOSHIYUKI KIMURA¹, YOSHIKAZU HASEGAWA¹ AND TADASHI SUZUKI²

¹Gunma Museum of Natural History, 1674-1 Kamikuroiwa, Tomioka, Gunma Prefecture 370-2345, Japan (e-mail: kimura@gmnh.pref.gunma.jp)

²5-2 Jiyugaoka, Iwaki, Fukushima Prefecture 970-8033, Japan

Received April 8, 2021; Revised manuscript accepted August 12, 2021; Published online October 1, 2022

Abstract. The *Isanacetus*-group is one of the most enigmatic groups of cetaceans. Although their phylogeny is still controversial, many previous studies suggested that they are a paraphyletic group of baleen whales, including an ancestor of Balaenopteridae and Eschrichtiidae. A new fossil from an *Isanacetus*-group baleen whale has been recovered from the Minamishirado Formation (latest early Miocene, Burdigalian), Iwaki, Fukushima Prefecture, Japan. The specimen consists of a cranium, mandible, and postcranial elements, including cervical, thoracic, and lumbar vertebrae, scapula, ulna, and ribs. We describe and diagnose the specimen as a new genus and species, *Jobancetus pacificus*. A unique combination of morphological characters characterized the specimen, e.g. frontals forming a triangular elevated plateau at the vertex, sharp, and well-developed transverse crest on the supraorbital process of frontal, sagittal crest formed by frontals and parietals, and large squamosal fossa, which is posteriorly extended well beyond the level of the posterior surface of the occipital condyle. Phylogenetic analysis under equal weighting suggests that *J. pacificus* is a stem group of Pligogulae, whereas the phylogenetic analyses under implied weightings suggest that *J. pacificus* is a stem group of Balaenopteridae + Eschrichtiidae. The discovery of *J. pacificus* expands our knowledge of the enigmatic *Isanacetus*-group.

ZooBank registration: urn:lsid:zoobank.org:pub:22716311-EE7E-4CE3-95DC-169975A1F479

Keywords: Cetacea, *Isanacetus*-group, Japan, *Jobancetus pacificus*, Miocene, Mysticeti

Introduction

The family Cetotheriidae was firstly proposed by Brandt (1872) as a subfamily Cetotheriinae in Balaenopteridae, and Miller (1923) raised it to the family rank. Cabrera (1926) recognized three groups within Cetotheriidae. Kellogg (1928, 1934) examined Cabrera's (1926) grouping recognizing two groups and named them as a first and second group. However, the monophyly of Cetotheriidae had long been questioned by many authors (e.g. Barnes *et al.*, 1985; Fordyce and Barnes, 1994). They were a so-called “wastebasket taxon” and widely regarded as a paraphyletic edentulous mysticete family lacking the apomorphies of other mysticete families (Fordyce and Barnes, 1994; Geisler and Luo, 1996; Kimura and Ozawa, 2002).

Kimura and Ozawa (2002) tentatively named the *Isanacetus*-group for Cetotheriidae, excluding the taxonomic group closely related to *Cetotherium*. The *Isanacetus*-group corresponds to Kellogg's (1928, 1934) second group (Kimura and Ozawa, 2002; Kimura and Hasegawa,

2010). Bouetel and Muizon (2006) discussed a phylogeny of Cetotheriidae and redefined it as Cetotheriidae *sensu stricto*, referring to a monophyletic group of cetaceans that are closely related to *Cetotherium*. They also used the term “Cetotheriidae” *sensu lato* to refer to taxa included in the paraphyletic family Cetotheriidae *sensu* Simpson (1945), McKenna and Bell (1997), and Rice (1998). Thus, under the definition of Bouetel and Muizon (2006), the *Isanacetus*-group is a group of cetaceans that belongs to “Cetotheriidae” *sensu lato*, excluding Cetotheriidae *sensu stricto* (Kimura and Hasegawa, 2010).

In recent studies, the *Isanacetus*-group has also been referred to as *Isanacetus*-group cetothere (*sensu lato*) (El Adli *et al.*, 2014), ‘cetotheres’ (Bisconti *et al.*, 2013), ‘cetotheres’ *sensu lato* or “Cetotheres” *sensu lato* (Marx, 2011; Boessenecker and Fordyce, 2015a, b; Marx *et al.*, 2016, 2017; Tanaka *et al.*, 2018), Cetotheriidae *sensu lato* (Bisconti *et al.*, 2013; Boessenecker and Fordyce, 2017; Tsai and Fordyce, 2016), basal thalassotherians (Bisconti *et al.*, 2013), thalassotherian stem group (Bisconti *et al.*, 2013), Thalassotherii *sedis mutabilis* (Bisconti *et al.*,

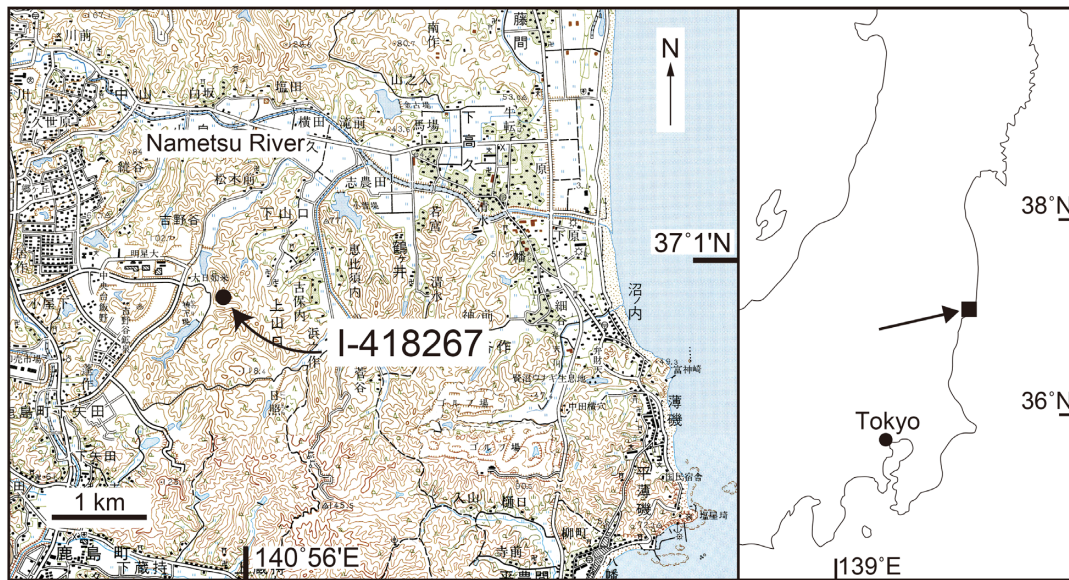


Figure 1. Locality of *Jobancetus pacificus*, gen. et sp. nov., I-418267. The base map is from the “Taira” and “Onahama” 1:50,000 topographic maps published by the Geospatial Information Authority of Japan.

2013), stem-balaenopteroid (Marx and Fordyce, 2015), and stem Balaenopteroidea (Marx and Fordyce, 2016). Following Kimura and Ozawa (2002), we will tentatively use the term *Isanacetus*-group until the taxonomic group is formally defined and named. Also, we will use the terms “Cetotheriidae” and “Cetotheriidae *sensu lato*” to refer to Cetotheriidae *sensu stricto* (*sensu* Bouetel and Muizon, 2006) and a group of cetaceans of Cetotheriidae + *Isanacetus*-group, respectively.

Cetotheriidae and *Isanacetus*-group have been believed to be closely related to the crown Mysticeti, and several lineages of modern Mysticeti were originated from the descendant of them (e.g. Marx *et al.*, 2016). Therefore, they are quite important for deciphering the evolutionary history of modern cetaceans. Whereas the concept of Cetotheriidae was recently well established (Fordyce and Marx, 2013; Marx *et al.*, 2019), that of *Isanacetus*-group is still controversial, and they remain one of the most enigmatic cetacean groups.

A skeleton of *Isanacetus*-group was discovered by Katsunori Funayama at a road-cut exposure near Iwaki Koyo High School, Iwaki City, Fukushima Prefecture, in September 1995 (Figure 1). This fossil was recovered in October 1995 and prepared by the Iwaki City Board of Education. The purpose of the present paper is to describe and diagnose the specimen.

Methods

To investigate the evolutionary relationship of *Jobance-*

tus pacificus, we performed a phylogenetic analysis using the matrix of Tanaka *et al.* (2020a), which was derived from the matrix of Marx *et al.* (2017). With the addition of *J. pacificus*, the final matrix consists of 100 operational taxonomic units and 273 morphological characters. Recently, Kimura and Hasegawa (2021) revised the coding of *Joumocetus shimizui* based on the newly found material (GMNH-PV-3456). We incorporated it into our matrix. Following Tanaka *et al.* (2020a), phylogenetic analysis was performed using TNT version 1.5 (Goloboff and Catalano, 2016) using the New Technology Search with recover minimum length tree = 1000 times. All the characters were treated as unordered and unweighted. The analysis was performed with a backbone constraint tree of modern taxa based on the molecular tree by McGowen *et al.* (2009). To assess the effect of the missing entries, we conducted the TNT analysis under equal and also implied weighting ($K = 3, 6, 9$).

Institutional Abbreviations.—GMNH, Gunma Museum of Natural History, Tomioka, Gunma, Japan; I, Iwaki City Board of Education, Iwaki, Fukushima, Japan; MSM, Museum of Southern Jutland, Department Natural History and Palaeontology, Gram, Denmark; NMR, Natuurhistorisch Museum Rotterdam, the Netherlands.

Systematic paleontology

Cetacea Brisson, 1762
Neoceti Fordyce and Muizon, 2001
Mysticeti Flower, 1864

Chaeomysticeti Mitchell, 1989

Incertae familiae

Jobancetus gen. nov.

ZooBank lsid: urn:lsid:zoobank.org:act:03B2C75F-F3D7-426A-B191-9BD25883EDF4

Type and only known species.—*Jobancetus pacificus*, sp. nov.

Diagnosis.—As for the type and only species.

Etymology.—*Jobancetus* refers to an old Japanese district named ‘Joban’ [area including a southern part of Fukushima Prefecture and northern part of Ibaraki Prefecture]; ‘cetus’ is Latin for whale.

Jobancetus pacificus sp. nov.

Figures 2–9

ZooBank lsid: urn:lsid:zoobank.org:act:D6E21463-0C7D-4B84-A491-B9F48A3B36E1

Holotype.—I-418267, nearly complete cranium (tympanic bullae and periotics are in situ), both mandibles, and postcranial elements including cervical, thoracic, and lumbar vertebrae, scapula, ulna, and ribs, found in 1995. The holotype specimen is owned by Iwaki City Board of Education and housed in Iwaki City Coal and Fossil Museum, Iwaki, Fukushima, Japan.

Type Locality.—The holotype originates from a road-cut exposure near Iwaki Koyo High School, Iwaki City, Fukushima Prefecture, Japan (latitude 37°0′57″N, longitude 140°55′37″E; Figure 1).

Horizon and Age.—Minamishirado Formation, Shirado Group, latest early Miocene, Burdigalian. The Minamishirado Formation is divided into two parts (lower and upper part). The lower part consists of non-marine to brackish mudstone and sandstone, and the upper part consists of marine fine-grained sandstone. The holotype was found from the lower part of the Minamishirado Formation. Fission track dating of the tuff layer in the lower part of the Minamishirado Formation yielded geological age of 15.9 ± 0.7 Ma (1 σ) (Kubo *et al.*, 2002). According to the diatom biostratigraphy, Minamishirado Formation is correlated to the upper part of the *Crucidentricula kanayae* Zone (NPD 3A: 16.5–16.3 Ma) (Koizumi, 1985, 1986; Yanagisawa and Akiba, 1998; Kubo *et al.*, 2002; Sudo *et al.*, 2005).

Etymology.—The species name reflects the occurrence of the holotype specimen in the Pacific Ocean and also reflects the Iwaki Koyo High School [yo meaning the Pacific Ocean].

Diagnosis.—*Jobancetus pacificus* can be identified from all other *Isanacetus*-group by having unique com-

ination of the following morphological characters: ascending processes of premaxillae and maxillae extending posteriorly to the level of the middle of the orbit, nasals elongated and its lateral edges being almost paralleled, frontals forming a triangular elevated plateau at the vertex, sharp and well-developed transverse crest on the supraorbital process of frontal, sagittal crest formed by frontals and parietals, large squamosal fossa, which is posteriorly extended well beyond the level of the posterior surface of the occipital condyle, slender and elongate zygomatic process of squamosal, which directs anteriorly and slightly laterally, large basioccipital crest, ventrally protruded angle of mandible, two longitudinal ridges on the ventral surface of the horizontal ramus, large foramen transversarium in axis vertebra.

Jobancetus can be distinguished from *Atlantocetus*, *Diorocetus*, *Isanacetus*, *Parietobalaena*, and *Taikicetus* by having sharp and well-developed transverse crest on the supraorbital process of frontal, sagittal crest formed by frontals and parietals, large squamosal fossa, which is posteriorly extended well beyond the level of the posterior surface of occipital condyle; further differs from *Atlantocetus* and *Diorocetus* by having ascending processes of premaxillae and maxillae extending posteriorly to the level of the middle of the orbit; further differs from *Atlantocetus* by having lateral edges of nasals being almost parallel. Also, it differs from *Cophocetus*, *Titanocetus*, *Pinoceetus*, and *Uranocetus* by having sharp and well-developed transverse crest on the supraorbital process of frontal; further differs from *Titanocetus* by having anteriorly pointed apex of the supraoccipital and ventrally protruded angle of mandible; further differs from *Uranocetus* by having lateral edges of nasals being almost parallel and by lacking circular outline of the mandibular condyle in the posterior view and transversally thickened apex of coronoid process of the mandible. By having frontals forming a triangular elevated plateau at the vertex, *Jobancetus* differs from *Atlantocetus*, *Cophocetus*, *Diorocetus*, *Isanacetus*, *Parietobalanea*, *Pelocetus*, *Pinocetus*, *Taikicetus*, and *Titanocetus*. *Jobancetus* differs from *Aglaocetus* by having anterior border of mandibular foramen located posterior to level of apex of coronoid process; differs from *Mauicetus* by having a posterior apex of nuchal crest posterior to the occipital condyle; differs from *Imerocetus* by having sharp and well-developed transverse crest on the supraorbital process of frontal. Unlike *Atlantocetus*, *Halicetus*, *Isocetus*, and *Pelocetus*, *Jobancetus* has transverse process of atlas dorsoventrally wide and located on the level of the center of the articular fovea. *Isocetus* also differs from *Jobancetus* by having mandibular condyle round and transversely wide.

Jobancetus also differs from *Piscocetus* and *Tiphyocetus* by having large squamosal fossa, which is posteriorly



Figure 2. *Jobancetus pacificus*, gen. et sp. nov., I-418267, holotype. Photographs of the cranium in **A**, dorsal; **B**, ventral; **C**, posterior, and **D**, right lateral views. The hatched area represents a reconstructed part of the bone.

extended well beyond the level of the posterior surface of occipital condyle; further differs from *Tiphycetus* by lacking a convexly curved ventral surface of squamosal.

Jobancetus has a slender and elongate zygomatic process of squamosal, which directs anteriorly and slightly laterally, differing from *Cophocetus*, *Otradnocetus*, *Pis-*

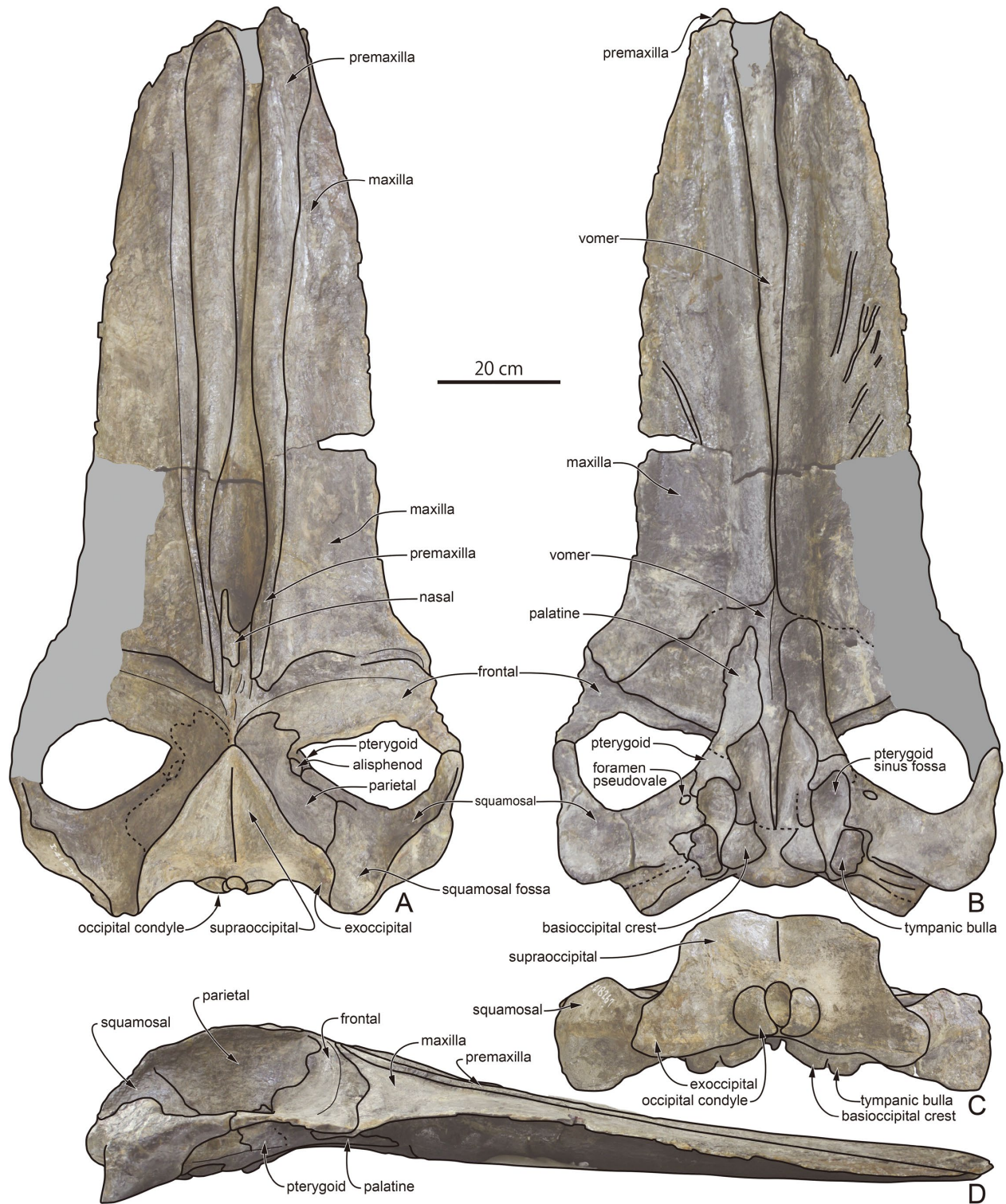


Figure 3. *Jobancetus pacificus*, gen. et sp. nov., I-418267, holotype. Interpretive illustration of the cranium in **A**, dorsal; **B**, ventral; **C**, posterior, and **D**, right lateral views. The gray area represents a reconstructed part of the bone.



Figure 4. *Jobancetus pacificus*, gen. et sp. nov., I-418267, holotype. Photograph (left) and interpretative illustration (right) of vertex of the cranium in dorsal view.

cocetus, and, *Taikicetus*. *Jobancetus* further differs from *Otradonocetus* by having ascending processes of premaxillae and maxillae extending posterior to the level of the middle of orbit and by lacking the circular outline of the mandibular condyle in the posterior view. By having a large foramen transversarium of the axis, *Jobancetus* differs from *Cophocetus*, *Diorocetus*, *Halicetus*, *Isanacetus*, *Pelocetus*, and *Thinocetus*. *Jobancetus* also differs from *Thinocetus* by having posterolateral edge of the exoccipital located far posterior to the level of the posterior surface of the occipital condyle.

Description

Anatomical terminology generally follows Mead and Fordyce (2009). The cranium of the holotype is almost complete, except for the lateral portion of the base of the left maxilla and a part of the supraorbital process of the left frontal (Figures 2, 3). The condylobasal length is 1397+ mm, and its maximum transverse diameter at the zygomatic process of the squamosal is 703 mm. The total body length is estimated as 7.25 m, based on the equation for the stem Balaenopteroidea developed by Pyenson and Sponberg (2011). In lateral view, the general dorsal pro-

file of the rostrum is almost straight.

At the vertex, the posterior extremities of the medial rostral elements (maxilla, premaxilla, and nasal) are slightly broken off. Thus, the dorsal surface of the corresponding part of the frontals, which were originally covered by the maxilla/premaxilla/nasal, is exposed (Figure 4), indicating the original position of the posterior end of the medial rostral elements. The medial rostral elements originally extend posteriorly to the level of the middle of the orbit. The distance between the medial rostral elements and the apex of the supraoccipital shield is *ca.* 40 mm.

The epiphysial fusion is initiated at the anterior cervical vertebra (Kato, 1988; Costa and Simões-Lopes, 2012; Moran *et al.*, 2015). In I-418267, only the anterior epiphyses of the atlas, axis and 3rd cervical vertebrae and the posterior epiphysis of the atlas are fused with the centrum, and all other epiphyses of the cervical vertebrae are unfused, suggesting that the animal was a young individual.

Premaxilla.—The premaxilla widens anteriorly and is widest at the level of the anterior end of the maxilla: 87 mm and 71 mm for transverse width of the left and right premaxillae, respectively. Along the margin of the narial fossa, the premaxilla becomes transversely narrow.

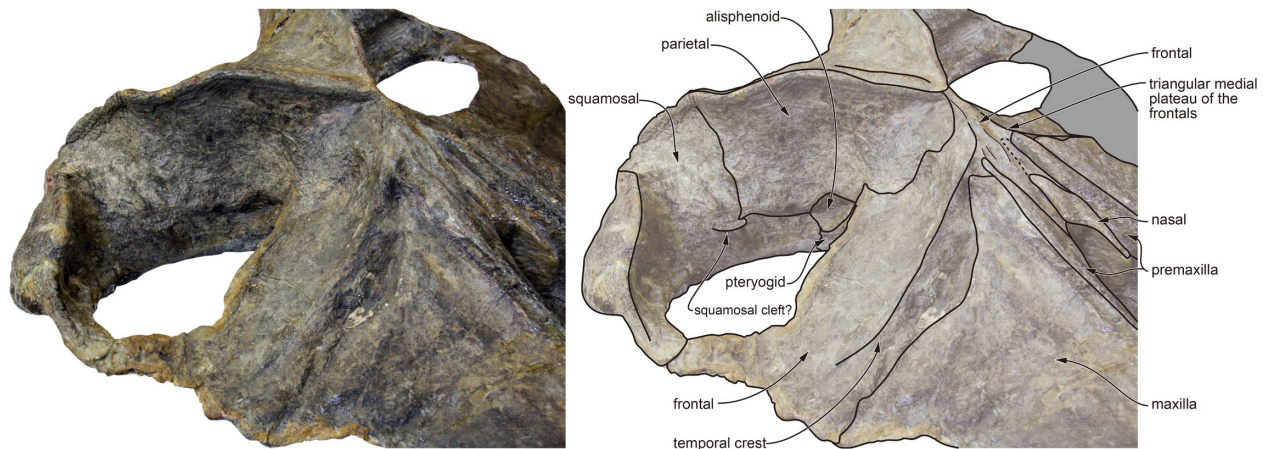


Figure 5. *Jobancetus pacificus*, gen. et sp. nov., I-418267, holotype. Photograph (left) and interpretive illustration (right) of the cranium in oblique anterolateral view.

The ascending process of the premaxilla is transversely narrow and almost parallel-sided, which is clearly in contrast to that of Cetotheriidae; the premaxilla of the latter narrows markedly posteriorly along the nasal. As stated above, the remains suggest the posterior extremity of the premaxilla extended posteriorly to the level of the middle of the orbit and ends at the posterolateral corner of the nasal.

Maxilla.—The rostral part of the maxilla is relatively slender, and its lateral margin gently tapers toward the anterior extremity. The dorsal surface of the rostral part of the maxilla slopes gradually downward laterally. Due to the poor preservation, the morphology of the antorbital notch and the dorsal infraorbital foramina is unknown. Though the posterior-most portion of the maxillae are damaged and its original shape is unclear, the remains suggest that the ascending process of the maxilla was broadly triangular and extends at least to the level of the middle of the orbit (Figure 4). In lateral view, the lateral edge of the maxilla is dorsoventrally thin. The ventral surface of the maxilla is gently concave, except for the palatal keel. Lateral to the palatal keel, the ventral surface carries a series of anterolaterally oriented shallow grooves for nutrient arteries for the baleen.

Nasal.—The left nasal is preserved, but the right one is missing, and the frontal is exposed in the corresponding area. Both the anterior and posterior portion of the left nasal are missing, and the preserved anteroposterior length of the left nasal is 113 mm. The exposed dorsal surface of the frontal, formerly covered by the nasal, suggests that the nasal was originally at least 185 mm in length (*ca.* 13 percent of the condylobasal length). In dorsal view, the outline of the left nasal is anteroposteriorly elongated and rectangular. The lateral and medial borders

are straight and almost parallel-sided. This is clearly in contrast to the triangular outline of the nasals in Cetotheriidae, e.g. *Metopocetus* (NMR 9991-07729), *Joumoceetus* (GMNH-PV-2401), and *Cetotherium* (Brandt, 1873).

Frontal.—The orbital margin of the right frontal is slightly damaged; the lateral part of the left supraorbital process is missing. The dorsal surface of the supraorbital process slopes gradually downward from the vertex to its orbital rim. The postorbital process elongates posterolaterally, making the posterior margin of the supraorbital process concave in dorsal view. The curved transverse temporal crest is remarkably developed and extends anterolaterally on the dorsal surface of the supraorbital process (Figure 5).

At the vertex, this crest forms a lateral margin of the triangular area, which was originally covered by the posterior extension of the medial rostral elements (a breakage exposed the dorsal surface of the frontal). A similar structure is also found in *Uranocetus* (MSM p 813), and Steeman (2009) named the structure as the triangular medial plateau of the frontals. Behind it, the opposite frontals, with parietals, meet on the midline of the cranium and form a sagittal crest. The transverse temporal crest continues to the sagittal crest medially.

In lateral view, the orbital rim is dorsoventrally thin and shallowly arched. In ventral view, the optic canal becomes abruptly broad from its origin toward the orbital rim at the lateral 1/3 of the supraorbital process. This may imply that the optic canal was ventrally closed along the medial part of the supraorbital process.

Vomer.—The vomer contributes to the floor of the mesorostral groove. In ventral view, the vomer is widely exposed between the maxillae and also the palatines. But due to the possible postmortem lateral displacement of

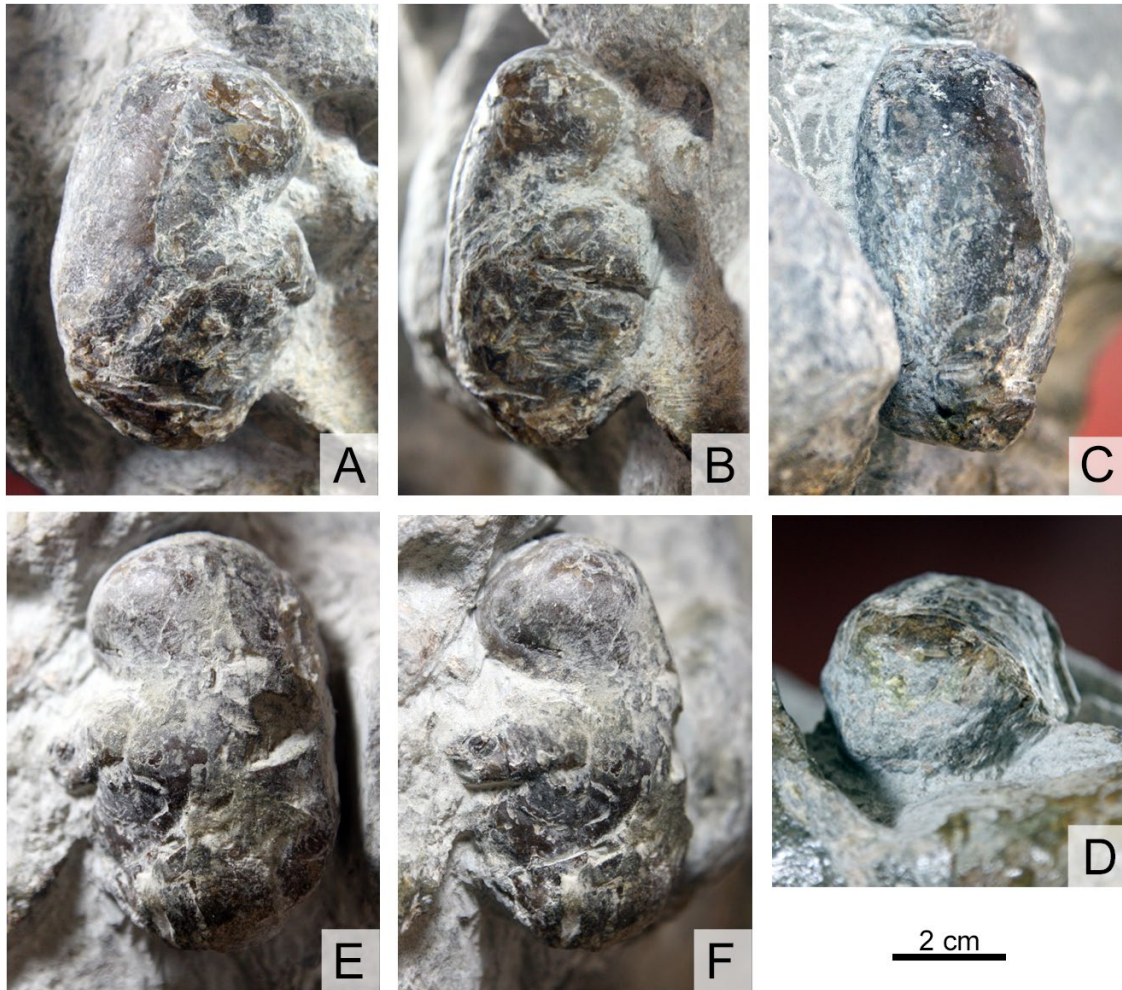


Figure 6. *Jobancetus pacificus*, gen. et sp. nov., I-418267, holotype. Left tympanic bulla in **A**, ventral; **B**, ventrolateral; **C**, ventromedial, and **D**, posterior views. Right tympanic bulla in **E**, ventral, and **F**, ventrolateral views.

the maxillae and the breakage of the medial part of the palatines, the exact extent of the exposure of the vomer along the midline of the cranium is unclear. The vomer extends posteriorly to the level of the anterior end of the tympanic bulla, and the vomerine crest also extends to the posterior end of the vomer. The vomerine crest is high and decreases its height posteriorly. The posterior portion of the vomer is transversely narrow and wedged between the medial lamina of the pterygoid.

Palatine.—The palatine is elongated anteroposteriorly, contacting the maxilla anteriorly and the pterygoid posteriorly. But due to the poor preservation, the maxilla-palatine and the palatine-ptyergoid sutures are unclear. As stated above, due to the breakage of the medial part of the palatines, the left and right palatines are widely separated by between exposure of the vomer.

Parietal.—Anterior to the apex of the supraoccipital,

the left and right parietals contact and form a part of the sagittal crest. It overrides the base of the supraorbital process of the frontal and extends forward to the level of the middle of the orbit. The parietal forms most of the lateral wall of the braincase. At the temporal surface, the parietal contacts the alisphenoid anteroventrally and the squamosal posteriorly and posteroventrally. In anterior view, the parietals of the temporal wall form a slight overhang at the nuchal crest.

Alisphenoid.—The alisphenoid is exposed on the temporal wall. It is small and ovoid in outline. It contacts with parietal dorsally, pterygoid anteroventrally, and squamosal posteroventrally (Figure 5).

Pterygoid.—In ventral view, the pterygoid is exposed between the palatine and the falciform process of the squamosal, but the palatine-ptyergoid suture is unclear. It does not contribute to the rim of the foramen pseudovale.

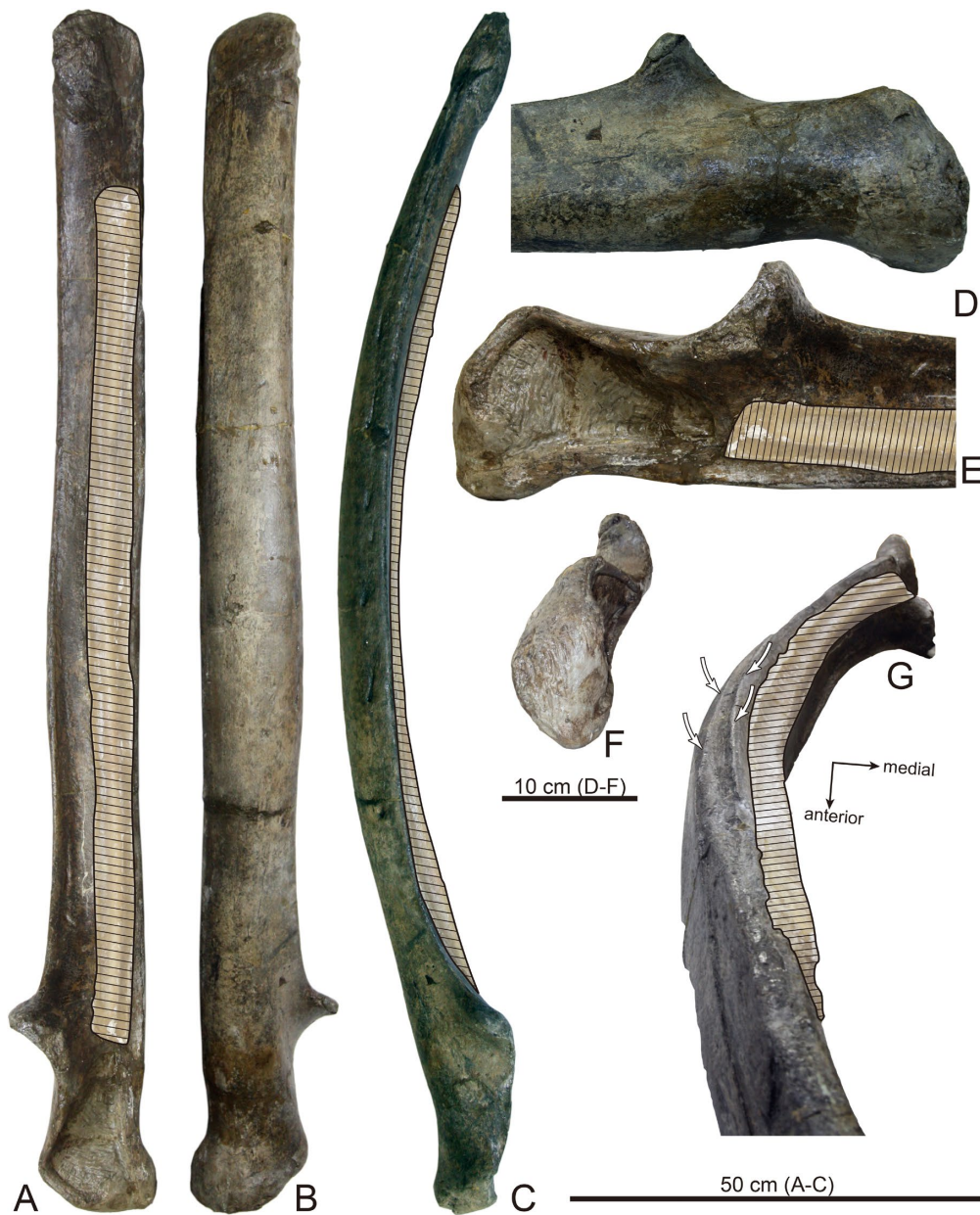


Figure 7. *Jobancetus pacificus*, gen. et sp. nov., I-418267, holotype. Left mandible in **A**, medial; **B**, lateral, and **C**, dorsal views. Posterior part of the left mandible in **D**, lateral; **E**, medial, and **F**, posterior views. **G**, anteroventral view of the left mandible. Arrows indicate the two longitudinal ridges on the ventral surface of the horizontal ramus. The hatched area indicates an area covered by resin.

The hamular process is small and extends posteromedially below and medial to the pterygoid sinus fossa. Dorsally, the pterygoid contacts the alisphenoid.

Squamosal.—The squamosal fossa is large and extends posteriorly beyond the level of the posterior surface of the occipital condyle. The slender and elongated zygomatic process is directed anteriorly and slightly laterally. The supramastoid crest of the zygomatic process is relatively low. At the base of the zygomatic process, the dorsome-

dial surface is almost flat. The transverse width between the left and the right apex of the zygomatic process is 703 mm. A possible squamosal cleft is found in the temporal surface of the left squamosal (Figure 5), but this interpretation should be considered with caution, because it is not confirmed in the right squamosal.

In lateral view, the ventral profile of the squamosal is slightly concave from the extremity of the postglenoid process to the apex of the zygomatic process. The base

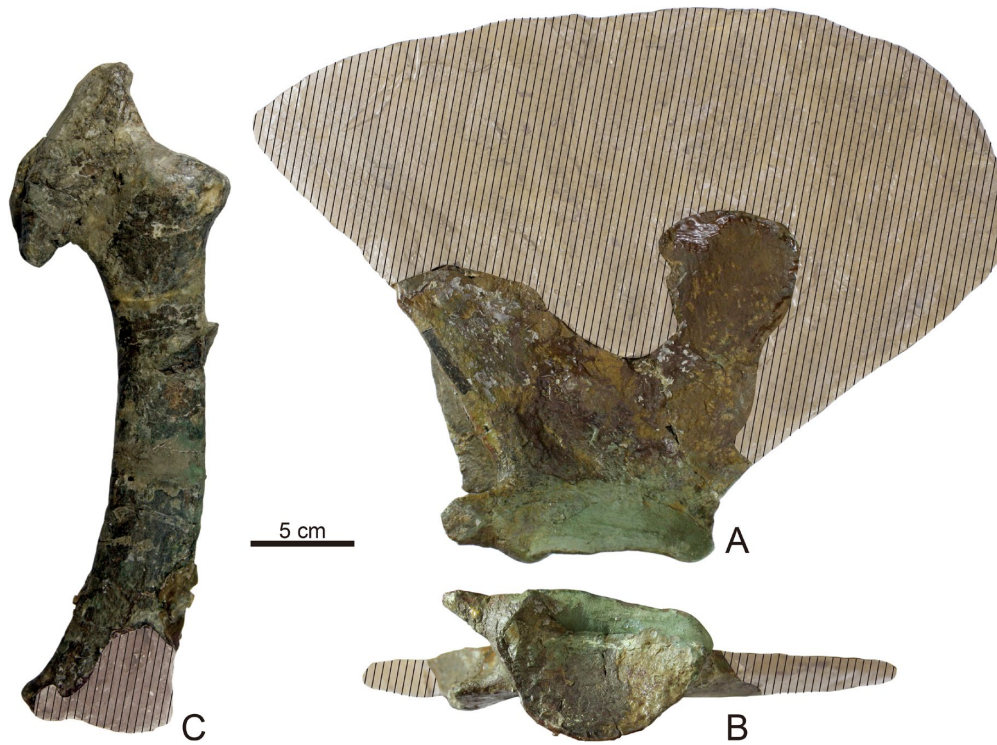


Figure 8. *Jobancetus pacificus*, gen. et sp. nov., I-418267, holotype. Right scapula in **A**, medial and **B**, ventral views. **C**, right ulna in lateral view. The hatched area indicates a reconstructed part of the bone.

of the postglenoid process is thickened anteroposteriorly. The postglenoid process is oriented ventrally and slightly posteriorly in lateral view. In posterior view, the postglenoid process projects laterally beyond the level of the lateral border of the exoccipital, and it is transversely wide. In ventral view, a falciform process contacts the posterior end of the pterygoid. A foramen pseudovale is fully enclosed within the falciform process.

Occipital.—In dorsal view, the supraoccipital extends anterior to the level of the anterior end of the zygomatic process of the squamosal. The supraoccipital forms a triangular outline, and the apex is acutely pointed anteriorly. The nuchal crest is well developed, and the supraoccipital shield is strongly concave. The nuchal crest is formed by the lateral margins of the supraoccipital, exoccipital, and abutting edges of the parietal and squamosal. It projects slightly laterally to create a small overhang of the parietal and is sinuous in dorsal view. The external occipital crest extends posteriorly from the apex of the supraoccipital.

The exoccipital is strongly extruded posteriorly and the posterolateral edge of the exoccipital extends posteriorly beyond the level of the posterior surface of the occipital condyle, thus the posterior surface of the exoccipital faces posteromedially. In ventral view, the basioccipital crest is bulbous and triangular in outline. The basioccipital crest

is large (transverse width: 71 mm, left; 72 mm, right) and reduces the transverse width of the median basicranial depression. The occipital condyle is large and reniform in outline in posterior view. The left and right condyle are well separated by the intercondylar notch. The foramen magnum is elliptical, and it is dorsoventrally higher (52 mm) than its width (36 mm).

Tympanic bulla.—Both tympanic bullae are preserved in situ. The anteroposterior length of the left and right bulla is 73 mm and 74 mm, respectively. In ventrolateral view, the anterior and posterior margin is convexly curved (Figure 6). The portion of the outer lip anterior to the lateral furrow is well inflated (anterolateral expansion: Bisconti, 2010). The sigmoid process is relatively small and directed dorsomedially and slightly posteriorly. The lateral furrow runs transversely across the lateral surface of the bulla. In ventromedial view, the profile of the bulla is almost rectangular in outline. The main ridge is low and extends from the posteroexternal angle to the level of the middle of its anteroposterior length.

Mandible.—The left mandible is almost complete, but the right one only consists of the anterior portion of the horizontal ramus (Figure 7). The total length of the left mandible is 1400 mm (in a straight line). The anterior part of the horizontal ramus is rotated around its axis, and the



Figure 9. *Jobancetus pacificus*, gen. et sp. nov., I-418267, holotype. Vertebrae in anterior view. **A**, 3rd and 4th cervical vertebrae; **B**, 5th cervical vertebrae with epiphysis of 4th cervical vertebra; **C**, complex of 6th and 7th cervical and 1st and 3rd thoracic vertebrae. T and L denote thoracic and lumbar vertebra, respectively.

medial surface faces mediodorsally. In dorsal view, the mandible is uniformly bowed laterally, and no reflection is present at the region of the coronoid process, unlike in balaenopterids. The medial surface of the horizontal ramus is almost flat. But, for a distance of at least 500 mm anterior to the apex of the coronoid process, a dorsal edge of the horizontal ramus is curved medially to create an overhang to its medial surface. The lateral surface of the horizontal ramus is flat at the anterior part and becomes convexly curved posteriorly. Ten mental foramina along the dorsolateral surface of the mandible are confirmed. A longitudinal crease is located at the medial surface of the anterior part of the horizontal ramus, and it is 122 mm long.

The coronoid process projects dorsally and laterally; its outline is almost triangular in lateral view. The height of the mandible at the apex of the coronoid process is 172 mm. The apex of the coronoid process is located 221 mm anterior to the posterior end of the occipital condyle. There is a well developed postcoronoid fossa. A mandibular foramen is large and triangular in shape even with a rounded anterior apex. The maximum transverse diameter of the condyle is 70 mm, and it occurs below the middle of its height. The angle of the mandible is robust and projects ventrally. The subcondylar furrow presents as a well-defined groove medially between the condyle and angle of the mandible.

The ventral margin of the cross-section of the horizontal ramus forms a well-defined angular edge. This sharply edged ventral margin is formed by two longitudinal ridges on the ventral surface of the horizontal ramus (Figure 7G). These ridges might represent an area for attaching the mylohyoid muscle (Pivorunas, 1977; Lambertsen, 1983; Kimura, 2002).

Scapula.—The right scapula is associated with the skeleton, but it only preserves a proximal part of it (Figure 8). The acromion is barely preserved, except its base, and it is dorsoventrally wide (84 mm). The coracoid process is small and directs anteromedially. The preserved length of the coracoid process is *ca.* 29 mm. The glenoid fossa is shallowly concave and roughly trapezoid in outline. Its anteroposterior diameter is 98 mm.

Ulna.—The right ulna is relatively well preserved (Figure 8C). The greatest length of the ulna measures 323 mm. The olecranon process is robust and roughly quadrangular in outline. The body of the ulna is bent posteriorly and widens distally. Its minimum anteroposterior diameter is 42 mm at the middle part of the body of the ulna.

Vertebrae.—Twenty-one vertebrae are associated with the skeleton (Figure 9). Measurements of the vertebrae are listed in Table 1.

Seven cervical vertebrae were recovered, and all are isolated. The atlas is the anteroposteriorly thickest among

Table 1. Measurements of vertebrae (in mm) of *Jobancetus pacificus* gen. et sp. nov., I-418267. Abbreviations: +, less than the true value; AH, anterior height of the centrum; AW, anterior width of the centrum; H, height at the neural spine; PH, posterior height of the centrum; PW, posterior width of the centrum; L, anteroposterior length of the centrum; C, cervical vertebra; T, thoracic vertebra; L, lumbar vertebra.

	AH	AW	PH	PW	L	H
C1	88	129	79	135	39	121
C2	80	123	73	98	29	96
C3	75	94	—	—	23	121
C4	—	—	84	91	19	19
C5	—	—	73+	88	21	21
C6	81	—	84	—	20	20
C7	—	86	—	—	22	22
T1	—	—	—	—	26	114
T2	72	92	81	101	32	142
T3	—	—	76	91	42	154+
T5	73	90	69+	97	46	197
T6	72	91	72	98	50	225
T8	76	90	75	105	58	257
T9	73	93	100	70	59	235
T11	97	73	74	95	68	246
T12	80	95	79	96	73	261
T13	81	91	76	99	78	256
T14	78	97	77	103	81	253
L1	81	93	81	100	84	256
L2	77	104	84	103	88	183+
L3	—	100	—	—	—	—

the cervical vertebrae, measuring 39 mm. The neural spine is relatively low, and the neural canal is higher than its width. Just dorsal to the anterior articular facet, a foramen is found at the base of the neural arch, and this foramen might be the passage of the vertebral artery. The anterior articular facets are concave and reniform in outline, transversely broadest at the middle of its height. The posterior articular facet is convex. The transverse process is dorsoventrally wide, and no foramen transversarium is found. Both anterior and posterior epiphyses are firmly ankylosed to the centrum.

The axis vertebra is incomplete, and the neural arch

is missing. The axis is transversely wide. The anterior articular facet is approximately reniform in outline. The odontoid process is broad and relatively low anteroposteriorly. The anterior epiphysis is ankylosed to the centrum, whereas the posterior one is not. The transverse processes project laterally and slightly posteriorly. A foramen transversarium is large and ovoid in outline, and it is wider than its height. The transverse width of the left and right foramen transversarium is 44 mm.

The third-fourth cervical vertebrae and the fifth-sixth cervical vertebrae are found as a single complex, respectively; however, no evidence exists that the bones were originally fused together. The anterior epiphysis of the third cervical vertebrae is ankylosed to the centrum, whereas all other epiphyses of the third to seventh cervical vertebrae are not ankylosed to the centrum. The outline of the centra of the cervical vertebrae appears roundly rectangular in the anterior/posterior view.

Eleven thoracic and three lumbar vertebrae are associated with the skeleton. Some of the vertebrae were found in their original undisturbed sequence. We identified that *J. pacificus* originally exhibited 14 thoracic vertebrae since the first and 14th thoracic vertebrae were found as a connection with the seventh cervical and first lumbar vertebrae by a matrix, respectively.

Discussion

Result of phylogenetic analysis.—In equal weighting, the analysis resulted in 2959 shortest trees with consistency index, 0.275; retention index, 0.734; tree length, 1315 steps. Fifty percent majority-rule consensus tree of the analyses is shown in Figure 10A. The result of the analysis suggests i) paraphyly of *Isanacetus*-group, ii) monophyly of Cetotheriidae, and iii) monophyly of the clade consisting of a part of *Isanacetus*-group + Cetotheriidae + Eschrichtiidae + Balaenopteridae. The assumption of the backbone tree constraints does not affect the resulting tree topology, and the same resulting tree topologies are suggested in the analysis with or without backbone tree constraints.

In our analysis under equal weighting, *Isanacetus*-group is recognized as a stem group of the clade comprising Cetotheriidae, Balaenopteridae and Eschrichtiidae. *Jobancetus pacificus* is placed as a basal member of the *Isanacetus*-group, which is clustered with *Aglaocetus moreni*, *Mauicetus parki*, and undescribed cetacean ZMT 67. Two synapomorphies support this clade: the tip of the postglenoid process is pointing ventrally in lateral view (Chr. 117), the exposure of the compound posterior process of the periotic, and the tympanic bulla on the lateral skull wall is absent or poorly defined (Chr. 186).

The results of analyses under implied weighting ($k =$

3, 6, 9) are essentially identical. The analyses of $k = 3$ resulted in 10 shortest trees with consistency index = 0.268, retention index = 0.724, tree length 118.76378 steps. Fifty percent majority-rule consensus tree of the analyses of $k = 3$ is shown in Figure 10B. The results under implied weighting of $k = 6$ and 9 are shown in the supplementary material. The results suggest i) monophyletic clade consisting of Cetotheriidae, Eschrichtiidae, Balaenopteridae, and *Isanacetus*-group excluding *Mauicetus* and ZMT 67 and ii) *Isanacetus*-group, excluding *Titanocetus*, *Mauicetus*, and ZMT 67, form a monophyletic clade with Balaenopteridae and Eschrichtiidae. The results suggest that *J. pacificus* is a stem group of Balaenopteridae + Eschrichtiidae. *Jobancetus pacificus* is included in the clade closely related to the clade of Balaenopteridae and Eschrichtiidae but not Cetotheriidae, and, in this respect, the results of implied weighting are inconsistent with that of equally weighting analysis. *Jobancetus pacificus* formed a clade with *Aglaocetus moreni*, and two synapomorphies support this clade: the lateral margins of the nasal are in parallel (Chr. 74), and the posterior apex of the nuchal crest is posterior to the level of the occipital condyle (Chr. 91).

In implied weighting analyses, *Titanocetus*, which has been regarded as a member of *Isanacetus*-group (e.g. Kimura and Hasegawa, 2010; Marx *et al.*, 2017), is clustered within the Cetotheriidae and therefore, the monophyly of Cetotheriidae is not supported. Two synapomorphies support this clade: the presence of the squamosal cleft (Chr. 109) and the facial sulcus on the compound posterior process of the periotic and the tympanic bulla partially or entirely floored by a posteroventral flange (Chr. 182), though the former is absent and the latter is unknown for *Titanocetus* (Bisconti, 2006). The phylogenetic position of the *Titanocetus* still remains unclear in our analysis and it should be further explored by future studies.

Phylogeny of Isanacetus-group.—In the past quarter-century, more than 50 papers published the result of the computer-assisted phylogenetic analysis providing insight into the phylogenetic relationships of *Isanacetus*-group, Cetotheriidae, Eschrichtiidae, and Balaenopteridae. However, regarding the phylogeny of the *Isanacetus*-group, a consensus has not been reached until now. This is also the case of our analyses. As stated above, our results of phylogenetic analyses under equally and implied weightings are inconsistent in the phylogeny of *Isanacetus*-group (Figure 11). Comparing the resulting tree topology with the temporal distribution of the included fossil records, there is a larger ghost lineage in the result of equally weighting analysis. In this respect, the results of implied weighting are more consistent with the fossil record.

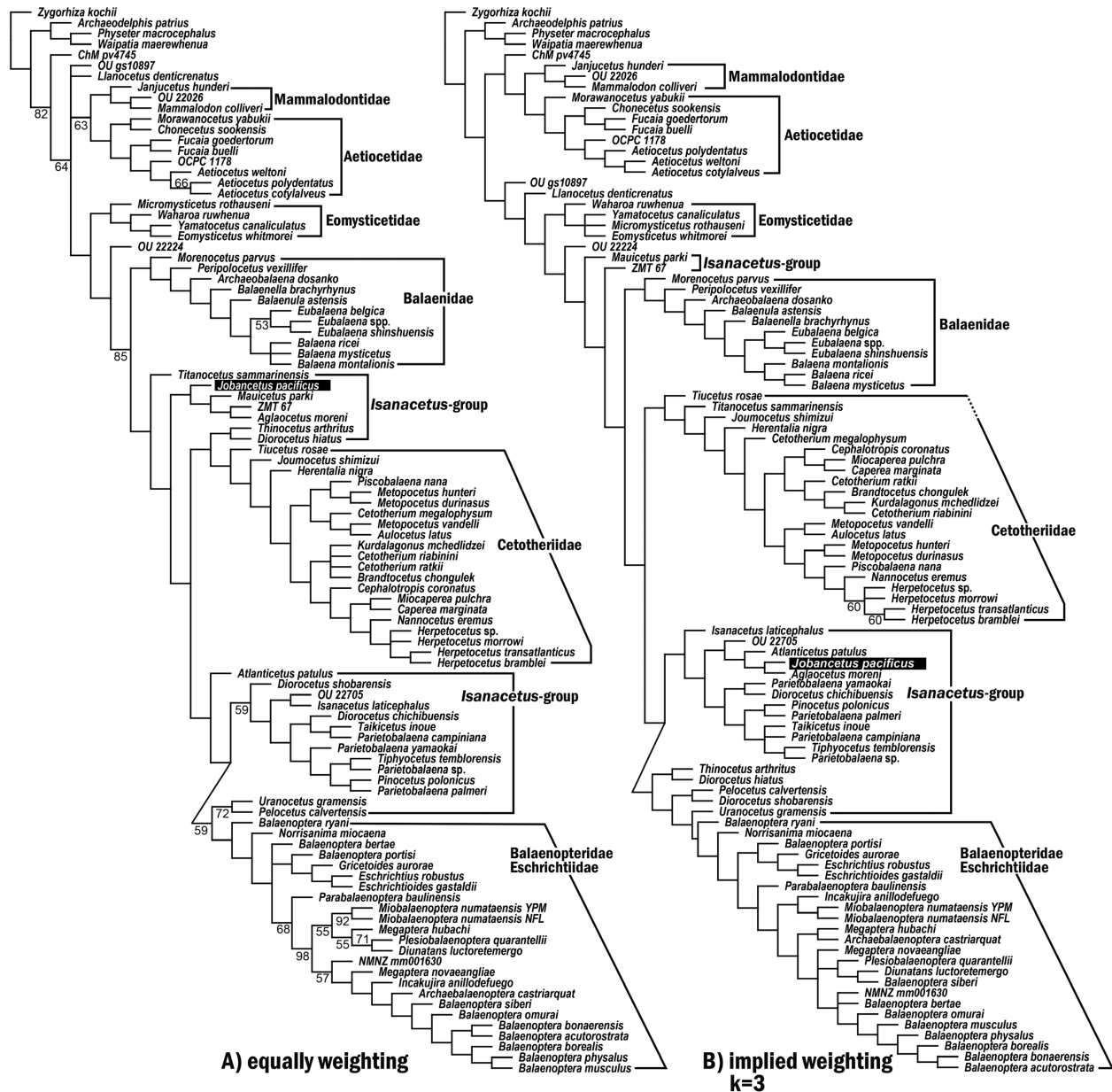


Figure 10. Fifty percent majority-rule consensus tree under equally and implied ($k = 3$) weighting analyses. Numbers at nodes indicate consensus frequency of the node in percent; the number at nodes supported 100% is omitted.

Only one clade within *Isanacetidae* is consistently supported in all our analyses, i.e., the clade consisting of *Parietobalaena* spp., *Diorocetus chichibuensis*, *Pinocetus polonicus*, *Taikicetus inouei*, and *Tiphycetus temblorensis*. In an equal weighting analysis, this clade is supported by seven synapomorphies: anteriormost point of the palatine located anterior to the level of the antorbital notch (Chr. 20), absence of the distinct ridge delimiting insertion surface of the tensor tympani on the medial side of the anterior process of the periotic (Chr. 160),

the caudal tympanic process of the periotic developed as a posteriorly extending triangular shelf pointing posterodorsally (Chr. 166), the shape of the aperture for the cochlear aqueduct is rounded with sharply defined dorsal margins (Chr. 171), the crista transversa is well developed and reaching the cerebral surface of the pars cochlearis (Chr. 176), anterior border of the proximal opening of the facial canal is continuous with the hiatus Fallopii and shaped like a fissure (Chr. 178), and the anterior border of the mandibular foramen is sharply triangular (Chr. 223).

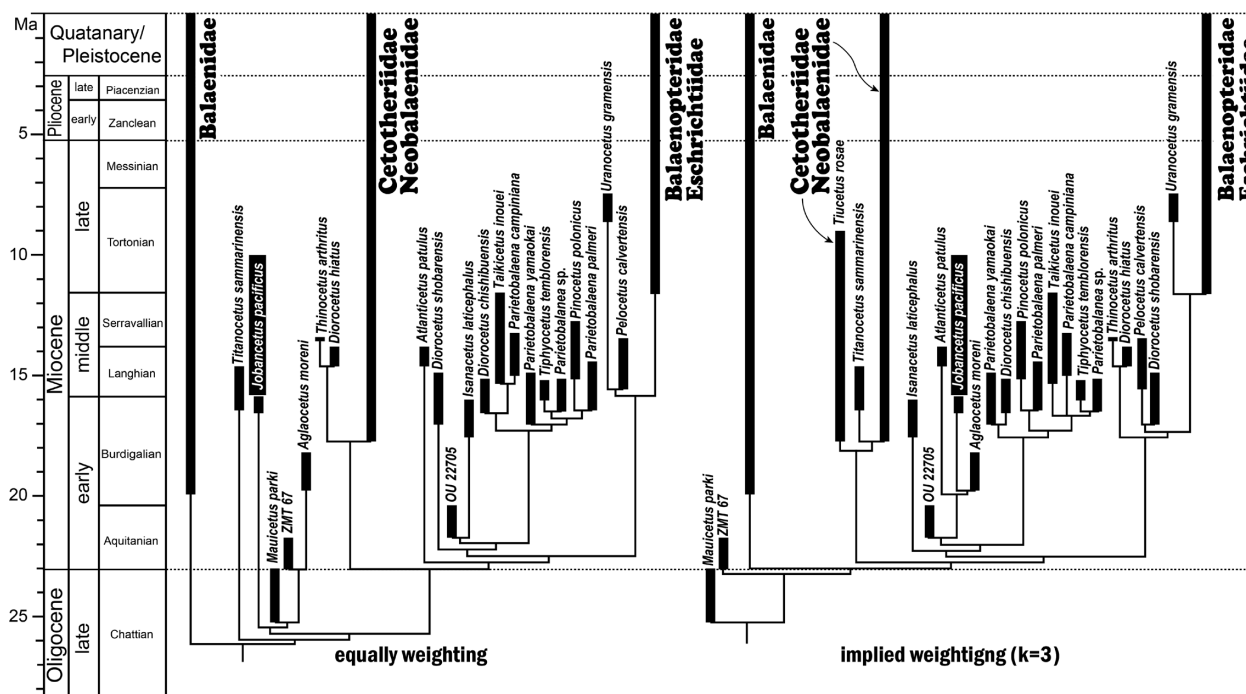


Figure 11. Simplified phylogenetic trees under the resulting tree of equal and implied ($k = 3$) weighting analyses with stratigraphic ranges. Stratigraphic range data were from Marx and Fordyce (2015), Buono *et al.* (2017), and Tanaka *et al.* (2018).

In all implied weighting analyses, this clade is supported by three synapomorphies: the presence of the squamosal cleft (Chr. 109) and the Chr. 160 and 223, which are also suggested in the equally weighting analysis. This clade might represent an unnamed lineage in *Isanacetus*-group, but the Bremer support index of the node is relatively low (2 and 0.00877 for equally and implied weighting analysis, respectively).

The *Isanacetus*-group ranges in age from the early Oligocene to the late Miocene, and they represent the highest diversity and disparity in the latest early to early middle Miocene. Though the phylogeny of *Isanacetus*-group remains unclear, it is suggested that the lineage leading to the Balaenopteridae and Eschrichtiidae originated from the *Isanacetus*-group during the early to middle Miocene based on the fossil records and the results of the phylogenetic analyses of the present (Figure 11) and previous studies (e.g. Kimura and Ozawa, 2002; Fordyce and Marx, 2013; Marx and Fordyce, 2016; Tsai and Fordyce, 2016; Boessenecker and Fordyce, 2017; Buono *et al.*, 2017; Bisconti *et al.*, 2020; Tanaka *et al.*, 2020b). However, their early Miocene record is quite limited and fails to document the evolutionary details leading to the high diversity and disparity of *Isanacetus*-group in the latest early/early middle Miocene. *Jobancetus pacificus* expands our knowledge of the *Isanacetus*-group, but *Isanacetus*-group is still one of the most enigmatic group

of cetaceans. The discovery of new, well-preserved fossil materials from the lower Miocene will be needed to document the details of the evolutionary history leading to the lineage of modern rorquals, humpback, and gray whales from *Isanacetus*-group.

Acknowledgments

We gratefully acknowledge the support by Iwaki City Foundation for Education and Culture and Iwaki City Board of Education. Constructive comments and suggestions from M. E. Steeman of The Museum of Southern Jutland and an anonymous reviewer considerably improved the quality of this work. We thank D. J. Bohaska, N. D. Pyenson, J. G. Mead, M. R. McGowen, J. J. Ososky, and D. P. Lunde of the National Museum of Natural History, Smithsonian Institution; M. Steeman and F. Osbaeck of MSM; O. Lambert of the Institut royal des Sciences naturelles de Belgique; and K. Post and B. Langeveld of NMR for facilitating access to specimens in their care. We also thank Y. Takakuwa of GMNH and S. Nabana of Iwaki City Coal and Fossil Museum for their help. This work was partly supported by JSPS KAKENHI Grant Numbers JP18K01110 to TK.

References

- Barnes, L. G., Domming, D. P. and Ray, C. E., 1985: Status of studies on fossil marine mammals. *Marine Mammal Science*, vol. 1, p. 15–53.
- Bisconti, M., 2006: *Titanocetus*, a new baleen whale from the middle Miocene of northern Italy (Mammalia, Cetacea, Mysticeti). *Journal of Vertebrate Paleontology*, vol. 26, p. 344–354.
- Bisconti, M., 2010: A new balaenopterid whale from the Late Miocene of the Stirone River, Northern Italy (Mammalia, Cetacea, Mysticeti). *Journal of Vertebrate Paleontology*, vol. 30, p. 943–958.
- Bisconti, M., Lambert, O. and Bosselaers, M., 2013: Taxonomic revision of *Isocetus depauwi* (Mammalia, Cetacea, Mysticeti) and the phylogenetic relationships of archaic ‘cetothere’ mysticetes. *Palaeontology*, vol. 56, p. 95–127.
- Bisconti, M., Munsterman, D. K., Fraaije, R. H. B., Bosselaers, M. E. J. and Post, K., 2020: A new species of rorqual whale (Cetacea, Mysticeti, Balaenopteridae) from the Late Miocene of the Southern North Sea Basin and the role of the North Atlantic in the paleobiogeography of *Archaebalaenoptera*. *PeerJ*, doi: 10.7717/peerj.8315.
- Boessenecker, R. W. and Fordyce, R. E., 2015a: Anatomy, feeding ecology, and ontogeny of a transitional baleen whale: a new genus and species of Eomysticetidae (Mammalia: Cetacea) from the Oligocene of New Zealand. *PeerJ*, doi: 10.7717/peerj.1129.
- Boessenecker, R. W. and Fordyce, R. E., 2015b: A new genus and species of eomysticetid (Cetacea: Mysticeti) and a reinterpretation of ‘*Mauicetus lophocephalus*’ Marples, 1956: Transitional baleen whales from the upper Oligocene of New Zealand. *Zoological Journal of the Linnean Society*, vol. 175, p. 607–660.
- Boessenecker, R. W. and Fordyce, R. E., 2017: A new eomysticetid from the Oligocene Kokoamu Greensand of New Zealand and a review of the Eomysticetidae (Mammalia, Cetacea). *Journal of Systematic Palaeontology*, vol. 15, p. 429–469.
- Bouetel, V. and Muizon, C. de., 2006: The anatomy and relationships of *Piscobalaena nana* (Cetacea, Mysticeti), a Cetotheriidae *s.s.* from the early Pliocene of Peru. *Geodiversitas*, vol. 28, p. 319–395.
- Brandt, J.-F., 1872: Über eine neue Classification der Bartenwale (Balaenoidea) mit Berücksichtigung der untergegangenen Gattungen derselben. *Bulletin de l’Académie Impériale des Sciences de St.-Petersbourg*, vol. 17, p. 113–124.
- Brandt, J.-F., 1873: Untersuchungen über die Fossilien und subfossilien Cetaceen Europa’s. *Mémoires de l’Académie Impériale des Sciences de Saint-Petersbourg*, vol. 20, p. 1–372.
- Brisson, M.-J., 1762: *Regnum animale in classes IX.: Distributum, sive Synopsis methocica sistens generalem animalium distributionem in classes IX, & duarum primarum classium, quadrupedum scilicet & cetaceorum, particularem divisionem in ordines, sectiones, genera & species. Editio altera auctior*, 296 p. Theodorum Haak, Leiden.
- Buono, M. R., Fernández, M. S., Cozzuol, M. A., Cuitiño, J. I. and Fitzgerald, E. M. G., 2017: The early Miocene balaenid *Morenocetus parvus* from Patagonia (Argentina) and the evolution of right whales. *PeerJ*, doi: 10.7717/peerj.4148.
- Cabrera, A., 1926: Cetaceos fósiles del Museo de La Plata. *Revista del Museo de La Plata*, vol. 29, p. 363–411.
- Costa, A. P. B. and Simões-Lopes, P. C., 2012: Physical maturity of the vertebral column of *Tursiops truncatus* (Cetacea) from Southern Brazil. *Neotropical Biology and Conservation*, vol. 7, p. 2–7.
- El Adli, J. J., Deméré, T. A. and Boessenecker, R. W., 2014: *Herpetocetus morrowi* (Cetacea: Mysticeti), a new species of diminutive baleen whale from the Upper Pliocene (Piacenzian) of California, USA, with observations on the evolution and relationships of the Cetotheriidae. *Zoological Journal of the Linnean Society*, vol. 170, p. 400–466.
- Flower, W. H., 1864: Notes on the skeletons of whales in the principal museums of Holland and Belgium, with descriptions of two species apparently new to science. *Proceedings of The Zoological Society of London*, vol. 1864, p. 384–420.
- Fordyce, R. E. and Barnes, L. G., 1994: The evolutionary history of whales and dolphins. *Annual Review of Earth and Planetary Sciences*, vol. 22, p. 419–455.
- Fordyce, R. E. and Marx, F. G., 2013: The pygmy right whale *Caperea marginata*: the last of the cetotheres. *Proceedings of the Royal Society B*, vol. 280, doi: 10.1098/rspb.2012.2645.
- Fordyce, R. E. and Muizon, C. de., 2001: Evolutionary history of cetaceans: a review. In: Mazin, J.-M. and Buffrénil, V. de eds., *Secondary adaptation of tetrapods to life in water*, p. 169–233. Friedrich Pfeil, München.
- Geisler, J. H. and Luo, Z., 1996: The petrosal and inner ear of *Herpetocetus* sp. (Mammalia; Cetacea) and their implications for the phylogeny and hearing of archaic mysticetes. *Journal of Paleontology*, vol. 70, p. 1045–1066.
- Geisler, J. H., McGowen, M. R., Yang, G. and Gatesy, J., 2011: A supermatrix analysis of genomic, morphological, and paleontological data from crown Cetacea. *BMC Evolutionary Biology*, vol. 11, p. 112–145.
- Goloboff, P. A. and Catalano, S. A., 2016: TNT version 1.5, including a full implementation of phylogenetic morphometrics. *Cladistics*, vol. 32, p. 221–238.
- Kato, H., 1988: Ossification pattern of the vertebral epiphyses in the southern minke whale. *Scientific Reports of the Whales Research Institute*, no. 39, p. 11–19.
- Kellogg, R., 1928: The history of whales—their adaptation to life in the water. *Quarterly Review of Biology*, vol. 3, p. 29–76 and p. 174–208.
- Kellogg, R., 1934: The Patagonian fossil whalebone whale, *Cetotherium moreni* (Lydekker). *Carnegie Institution of Washington Publication*, no. 447, p. 63–81.
- Kimura, T., 2002: Feeding strategy of an early Miocene cetothere from the Toyama and Akeyo Formations, central Japan. *Paleontological Research*, vol. 6, p. 179–189.
- Kimura, T. and Hasegawa, Y., 2010: A new baleen whale (Mysticeti: Cetotheriidae) from the earliest late Miocene of Japan and a reconsideration of the phylogeny of cetotheres. *Journal of Vertebrate Paleontology*, vol. 30, p. 577–591.
- Kimura, T. and Hasegawa, Y., 2021: Second report on the new material of *Joumocetus shimizui* from the Miocene Haraichi Formation, Annaka Group, Gunma, Japan. *Bulletin of the Gunma Museum of Natural History*, no. 25, p. 59–64. (in Japanese with English abstract)
- Kimura, T. and Ozawa, T., 2002: A new cetothere (Cetacea: Mysticeti) from the early Miocene of Japan. *Journal of Vertebrate Paleontology*, vol. 22, p. 684–702.
- Koizumi, I., 1985: Diatom biochronology for late Cenozoic Northwest Pacific. *Journal of Geological Society of Japan*, vol. 91, p. 195–211.
- Koizumi, I., 1986: Diatom biochronostratigraphy of the Neogene in the Joban coal-field, Northeast Japan—Yunagaya, Shirado, and Takaku Groups. In: Nakagawa, H., Kotaka, T. and Takayanagi, Y. eds., *Essays in Geology, Professor Nobu Kitamura Commemorative volume*, p. 175–191. Professor Nobu Kitamura Taikan Kinenjigyo-kai, Sendai.
- Kubo, K., Yanagisawa, Y., Toshimitsu, S., Banno, Y., Kaneko, N., Yoshioka, T. *et al.*, 2002: *Geology of the Kawamae and Ide district. Quadrangle Series, 1:50,000*, 136 p. Geological Survey of

- Japan, Tsukuba. (*in Japanese with English abstract*)
- Lambertsen, R. H., 1983: Internal mechanism of rorqual feeding. *Journal of Mammalogy*, vol. 64, p. 76–88.
- Marx, F. G., 2011: The more the merrier? A large cladistic analysis of mysticetes, and comments on the transition from teeth to baleen. *Journal of Mammalian Evolution*, vol. 18, p. 77–100.
- Marx, F. G. and Fordyce, R. E., 2015: Baleen boom and bust: a synthesis of mysticete phylogeny, diversity and disparity. *Royal Society Open Science*, vol. 2, doi: 10.1098/rsos.140434.
- Marx, F. G. and Fordyce, R. E., 2016: A link no longer missing: new evidence for the cetotheriid affinities of *Caperea*. *PLoS One*, doi: 10.1371/journal.pone.0164059.
- Marx, F. G., Lambert, O. and Muizon, C. de, 2017: A new Miocene baleen whale from Peru deciphers the dawn of cetotheriids. *Royal Society Open Science*, vol. 4, doi: 10.1098/rsos.170560.
- Marx, F. G., Lambert, O. and Uhen, M. D., 2016: *Cetacean Paleobiology*, 319 p. Wiley Blackwell, Chichester.
- Marx, F. G., Post, K., Bosselaers, M. and Munsterman, D. K., 2019: A large Late Miocene cetotheriid (Cetacea, Mysticeti) from the Netherlands clarifies the status of Tranatocetidae. *PeerJ*, doi: 10.7717/peerj.6426.
- McGowen, M. R., Spaulding, M. and Gatesy, J., 2009: Divergence date estimation and a comprehensive molecular tree of extant cetaceans. *Molecular Phylogenetics and Evolution*, vol. 53, p. 891–906.
- McKenna, M. C. and Bell, S. K., 1997: *Classification of mammals above the species level*, 631 p. Columbia University Press, New York.
- Mead, J. G. and Fordyce, R. E., 2009: The therian skull: a lexicon with emphasis on the odontocetes. *Smithsonian Contributions to Zoology*, no. 627, p. 1–248.
- Miller, G. S. J., 1923: The telescoping of the cetacean skull. *Smithsonian Miscellaneous Collections*, vol. 76, p. 1–70.
- Mitchell, E. D., 1989: A new cetacean from the Late Eocene La Meseta Formation, Seymour Island, Antarctic Peninsula. *Canadian Journal of Fisheries and Aquatic Sciences*, vol. 46, p. 2219–2235.
- Moran, M., Bajpai, S., George, J. C., Suydam, R., Usip, S. and Thewissen, J. G. M., 2015: Intervertebral and epiphyseal fusion in the postnatal ontogeny of cetaceans and terrestrial mammals. *Journal of Mammalian Evolution*, vol. 22, p. 93–109.
- Pivorunas, A., 1977: The fibrocartilage skeleton and related structure of the ventral pouch of balaenopterid whales. *Journal of Morphology*, vol. 151, p. 299–314.
- Pyenson, N. D. and Sponberg, S. N., 2011: Reconstructing body size in extinct crown Cetacea (Neoceti) using allometry, phylogenetic methods and tests from the fossil record. *Journal of Mammalian Evolution*, vol. 18, p. 269–288.
- Rice, D. W., 1998: Marine mammals of the world. Systematics and distribution. *The Society of Marine Mammalogy Special Publication*, no. 4, p. 1–231.
- Simpson, G. G., 1945: The principles of classification and a classification of mammals. *Bulletin of the American Museum of Natural History*, vol. 85, p. 1–350.
- Steeiman, M. E., 2009: A new baleen whale from the Late Miocene of Denmark and early mysticete hearing. *Palaeontology*, vol. 52, p. 1169–1190.
- Sudo, I., Yanagisawa, Y. and Ogasawara, K., 2005: Tertiary geology and chronostratigraphy of the Joban area and its environs, north-eastern Japan. *Bulletin of the Geological Survey of Japan*, vol. 56, p. 375–409. (*in Japanese with English abstract*)
- Tanaka, Y., Ando, T. and Sawamura, H., 2018: A new species of middle Miocene baleen whale from the Nupinai Group, Hikatagawa Formation of Hokkaido, Japan. *PeerJ*, doi: 10.7717/peerj.4934.
- Tanaka, Y., Furusawa, H. and Kimura, M., 2020b: A new member of fossil balaenid (Mysticeti, Cetacea) from the early Pliocene of Hokkaido, Japan. *Royal Society Open Science*, vol. 7, doi: 10.1098/rsos.192182.
- Tanaka, Y., Nagasawa, K. and Taketani, Y., 2020a: A new skull of an early diverging rorqual (Balaenopteridae, Mysticeti, Cetacea) from the late Miocene to early Pliocene of Yamagata, northeastern Japan. *Palaeontologia Electronica*, vol. 23, doi: 10.26879/1002.
- Tsai, C. H. and Fordyce, R. E., 2016: Archaic baleen whale from the Kokoamu Greensand: earbones distinguish a new late Oligocene mysticete (Cetacea: Mysticeti) from New Zealand. *Journal of the Royal Society of New Zealand*, vol. 2, p. 117–138.
- Yanagisawa, Y. and Akiba, F., 1998: Refined Neogene diatom biostratigraphy for the northwest Pacific around Japan, with an introduction of code numbers for selected diatom biohorizons. *Journal of Geological Society of Japan*, vol. 104, p. 395–414.

Author contributions

All authors contributed to this paper. T. K. was primarily responsible for the description and taxonomic aspects. Y. H. had discussions with T. K. T. S. carried out excavation and preparation of the holotype specimen.